



OBSERVATIONAL COSMOLOGY: OBSERVATIONAL FACILITIES

ASTRONOMY AND TELESCOPES

SOME BACKGROUND:

Until ~900 astronomy only in the visual bands and human eye only detector:

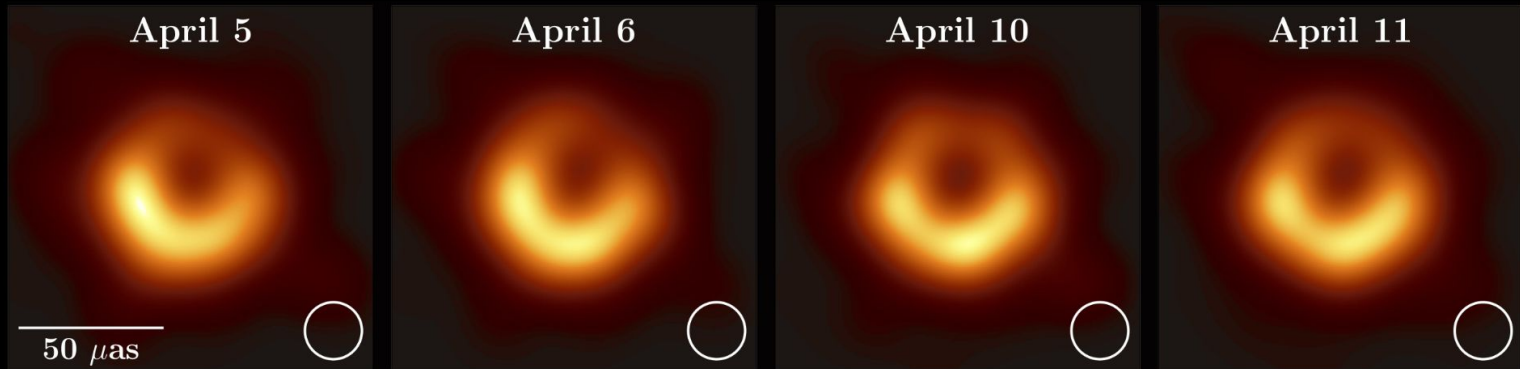
- λ : 4000-7000 A
- Resolution ~ arcmin
- Field Of View (FOV) ~ 160 deg
- Depth ~ +6 – +8 mag

Telescopes and detectors have revolutionized the field in terms of:

- Angular resolution
- Depth
- Surface Brightness
- Frequency Range

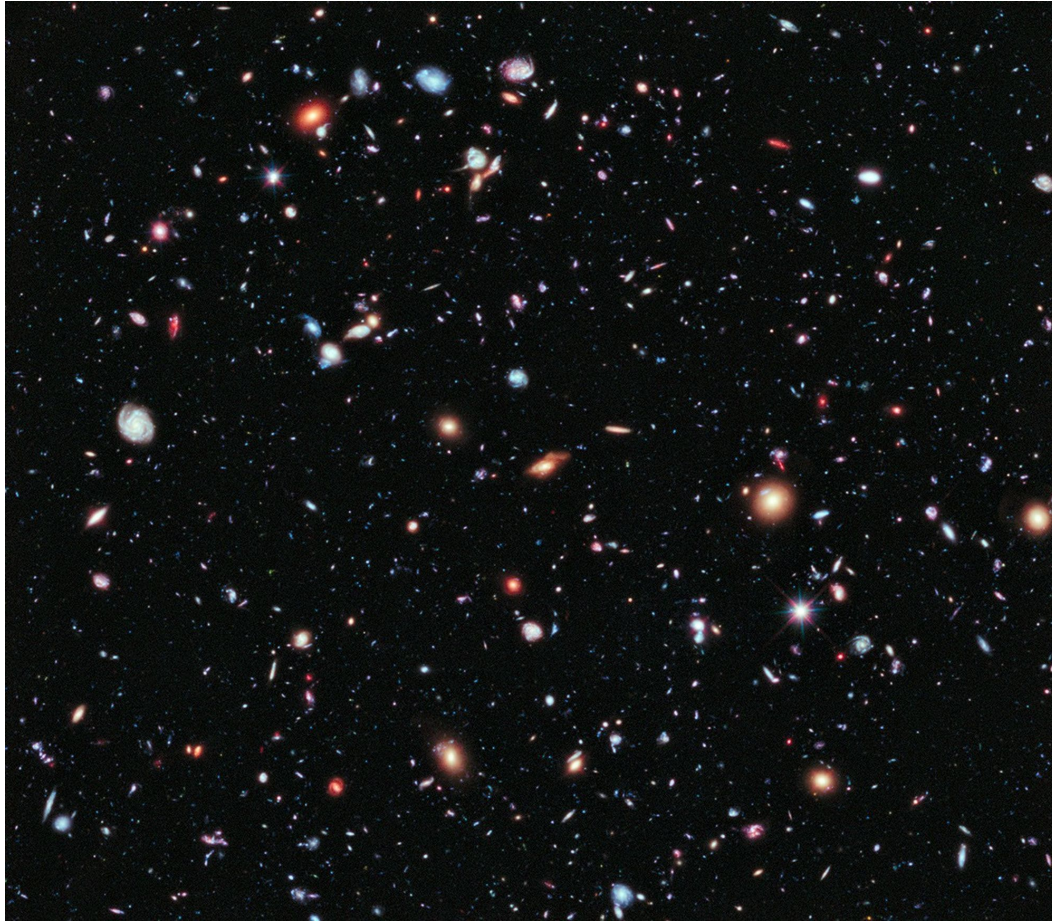
ASTRONOMY AND TELESCOPES

The nearby supermassive black hole in the Messier 87 galaxy



Event Horizon Telescope: $\sim 50 \mu$ arcsec

ASTRONOMY AND TELESCOPES



Hubble Extreme Deep Field ~
22.5 days of exposure time!! →
depth 31 mag

The XDF contains about 5,500 galaxies even within its smaller field of view (2x2 arcmin). The faintest galaxies are one ten-billionth the brightness of what the human eye can see.

ASTRONOMY AND TELESCOPES

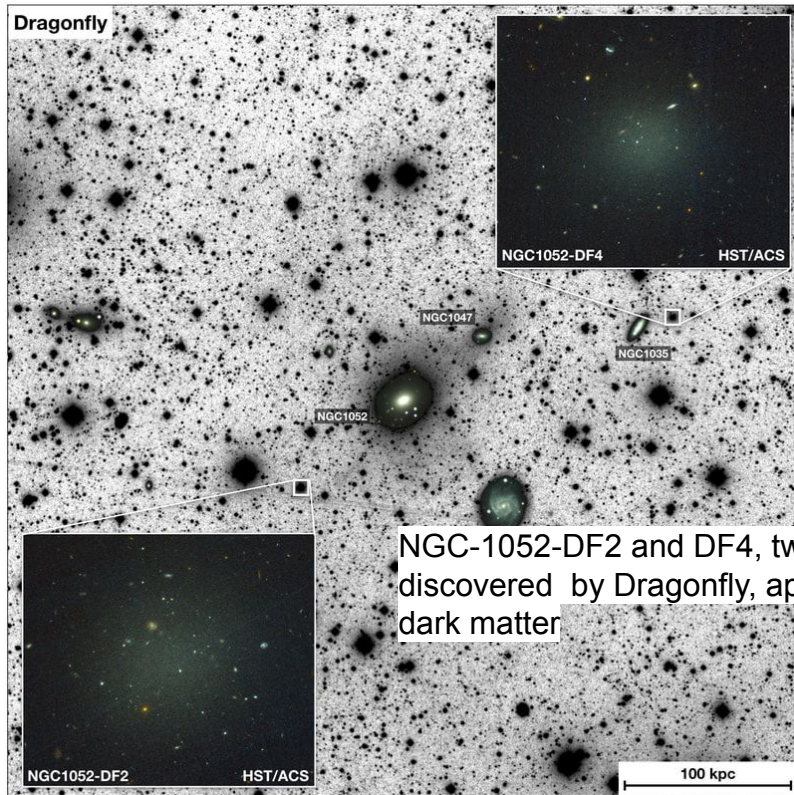


Dragonfly: is a telescope made up of a mosaic of Canon telephoto lenses on two mounts. The lenses all point to the same target in the sky: adding together all the images from the mosaic of lenses makes Dragonfly the equivalent of a one-metre telescope.

Dragonfly reached ~ 32 mag/arcsec !!
Significantly below current limit of 29 for normal telescope.

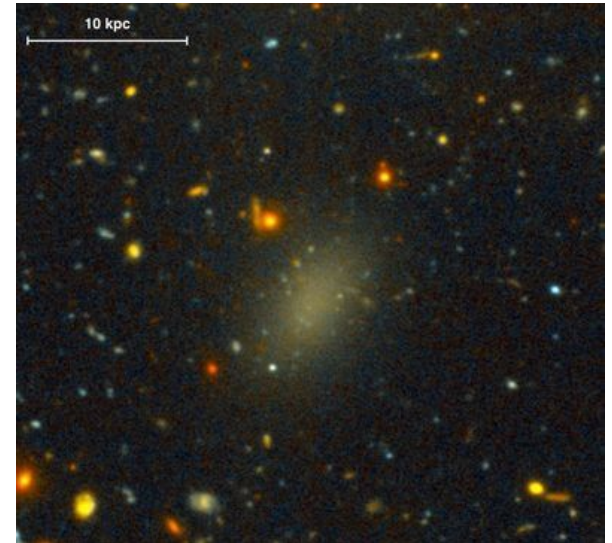
Dragonfly's unprecedented sensitivity to ultra-low surface brightness emission is driven by its exceptional control of scattered light and PSF wings.

ASTRONOMY AND TELESCOPES



NGC-1052-DF2 and DF4, two diffuse galaxies discovered by Dragonfly, apparently devoid of dark matter

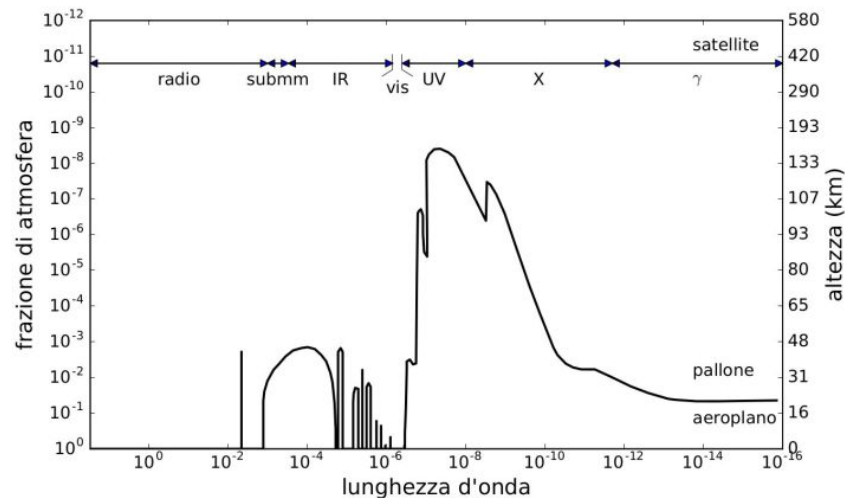
Using the W. M. Keck Observatory and the Gemini North telescope – both on Maunakea, Hawaii – a research team found a galaxy whose mass is almost entirely Dark Matter. Even though it is relatively nearby, astronomers had missed the galaxy, named Dragonfly 44, for decades because it is very dim. It was discovered just recently when the Dragonfly Telephoto Array observed a region of the sky in the constellation Coma.



FREQUENCY BANDS

banda	sotto-banda	λ
RADIO	(non oss.) radio microonde	$>30\text{m}$ $30\text{m} - 3\text{cm}$ $3\text{cm} - 1\text{mm}$
sub-mm		$1\text{mm} - 300\mu$
IR	FIR MIR NIR	$300\mu - 30\mu$ $30\mu - 5\mu$ $5\mu - 7000\text{\AA}$
ottico (visuale)		$7000\text{\AA} - 4000\text{\AA}$
UV	NUV soft UV EUV	$4000\text{\AA} - 3100\text{\AA}$ $3100\text{\AA} - 912\text{\AA}$ $912\text{\AA} - 100\text{\AA}$
X	soft X hard X	$100\text{\AA} - 10\text{\AA}$ $10\text{\AA} - 0.02\text{\AA}$
γ		$<0.02\text{\AA}$

λ	assorbimento	osservazioni
$> 300\text{m}$	plasma interplanetario	opaco
$> 30\text{m}$	ionosfera	(satellite)
$30\text{m} - 3\text{cm}$	finestra radio	da terra
$3\text{cm} - 1\text{mm}$	H_2O e O_2	alta montagna
$1\text{mm} - 10\mu$	H_2O , O_2 , CO_2	pallone o satellite
850μ e 450μ	finestre sub-mm	alta montagna
$10\mu - 7000\text{\AA}$	H_2O , molte finestre	alta montagna
$7000\text{\AA} - 3100\text{\AA}$	finestra ottica	da terra
$3100\text{\AA} - 912\text{\AA}$	O_3	satellite
$\sim 912\text{\AA}$	HI galattico	quasi opaco
$\lesssim 100\text{\AA}$	ionizzazione di stratosfera	satellite
$\lesssim 0.02\text{\AA}$	<i>scattering</i> Compton etc.	satellite
$E > 100\text{GeV}$	creazione di sciami	da terra



FREQUENCY BANDS

banda	oggetti visibili	meccanismi di emissione
radio	galassie, AGN, pulsar, SNR <i>HI</i>	sincrotrone, maser H_2O riga 21 cm
mm e sub-mm	Galassia CMB	bremstrahlung ($T \sim 10^4$ K) cosmologico
sub-mm	polveri nubi molecolari	emissione termica ($T \sim 50$ K) righe di emissione molecolari
FIR, MIR NIR	polveri nubi molecolari stelle K-M	emissione termica ($T \sim 50$ K) righe di emissione molecolari emissione termica ($T \sim 3000$ K)
ottico e NUV	stelle, AGN regioni <i>HII</i>	emissione termica fluorescenza
soft UV	stelle O-B corone stellari regioni <i>HII</i>	emissione termica ($T \sim 10^4$ K) bremstrahlung ($T \sim 10^6$ K) fluorescenza
EUV e X	corone stellari ammassi di galassie pulsar, binarie X, AGN e SNR	bremstrahlung ($T \sim 10^6$ K) bremstrahlung ($T \sim 10^8$ K) Compton inverso, sincrotrone
γ	GRB, AGN, pulsar	annichilazioni, decadimenti, sincrotrone, Compton inverso

INFORMATION CONTENT OF RADIATION

- The rate of arriving photons or flux
 - Constraints on luminosity given assumptions about emission geometry
 - Periodicity or variability in sources reveals physical nature
- The arrival direction or shape of source
 - Resolved versus unresolved- diffraction limit and atmospheric effects
 - Nature of resolved sources
- The photon energy distribution or spectrum
 - Composition of source – atomic features
 - Temperature of source- blackbody or bremsstrahlung
 - Line of sight relative velocity of source or redshift
- The polarization of the photons
 - Presence of magnetic fields with preferred direction
 - Scattering of dust grains

INFORMATION CONTENT OF RADIATION

- **The rate of arriving photons or flux**
 - **Constraints on luminosity given assumptions about emission geometry**
 - **Periodicity or variability of the sources reveals its physical nature**

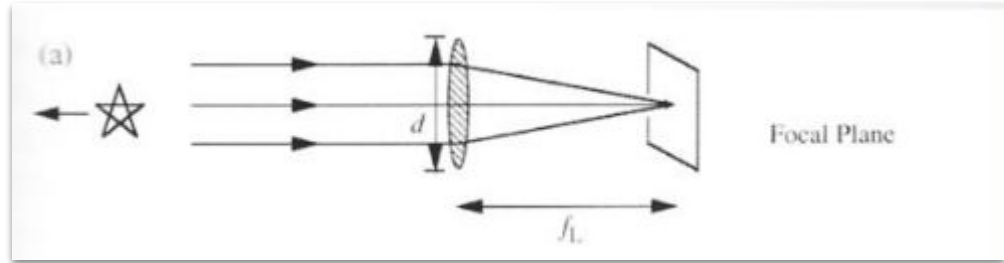
- **The arrival direction or shape of source**
 - **Resolved versus unresolved-diffraction limit and atmospheric effects**
 - **Nature of resolved sources**

- **The photon energy distribution or spectrum**
 - **Composition of source - atomic features**
 - **Temperature of source - blackbody or bremsstrahlung**
 - **Line of sight relative velocity of source or redshift**

OPTICAL/UV AND IR TELESCOPES

Image formation:

- Incoming parallel light from distant source focused to a point in the focal plane
 - Lens diameter d
 - Focal length f_L



- Focal ratio: $R = f_L / d$:
 - Low R ($\sim 4-5$) \rightarrow Fast optical systems: Good to detect extended, low surface brightness objects, since they focus the light on a small surface of the detector (focal plane irradiance: $E_p \propto 1 / R^2$ [W/m^2])
 - High R ($\sim 10-15$) \rightarrow Slow optical systems: more suited for high-resolution observations

OPTICAL/UV AND INFRARED

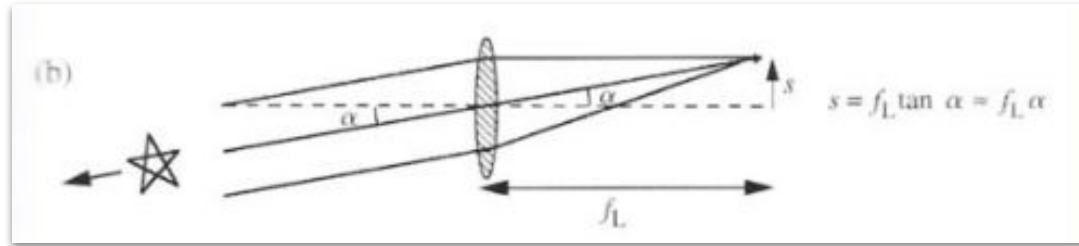
Image formation:

- Focal point varies with angle of incoming light

$$s = \tan \alpha f_L \approx \alpha f_L$$

- Plate scale:

$$P_s = \frac{\alpha}{s} = \frac{1}{f_L}$$



- Field of View (FoV):

$$\theta_{\max} = \arctan\left(\frac{d/2}{f}\right)$$

$$\text{FoV} = 2 \arctan\left(\frac{d}{2f}\right) \simeq 2 \cdot \frac{d}{2f} = \frac{d}{f}$$

OPTICAL/UV AND INFRARED

“Fast” and “slow” optical systems differ by their focal ratio: fast systems (low R) deliver higher irradiance per unit area on the detector and are optimal for extended, low surface brightness imaging (wide field survey), while slow systems (high R) provide higher angular magnification and are better suited for point-source and high-resolution applications.

Property	Fast system	Slow system
f-number	small	large
Surface brightness speed	high	low
FoV	wide	narrow
Aberrations	strong	weak

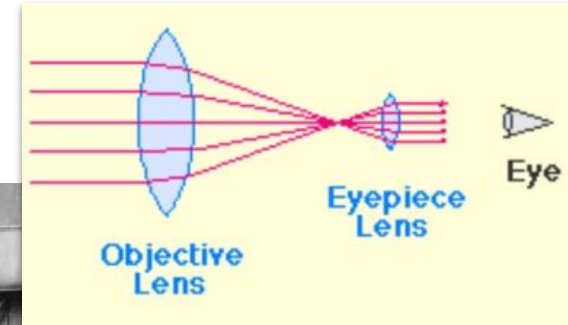
OPTICAL/UV AND INFRARED

Caratteristica	James Webb (JWST)	Euclid
Diametro Specchio	6.5 m	1.2 m
Distanza Focale	~131 m	24.5 m
Rapporto Focale	20	20
Campo Visivo (FoV)	Molto stretto: ~arcmin (Dettaglio)	Molto ampio: 0.57 deg ² (Survey)
Obiettivo Cosmologico	Prime stelle e galassie (profondità)	Materia/Energia Oscura (statistica)

TELESCOPE CONFIGURATION

Refractor Telescopes (lenses):

- **Pro: Aberration reduced or eliminated (beyond notice) using aspherical, achromatic, multiple lenses at objective and eyepiece.**
- **Cons:**
 - **large lenses are heavy and deform under their own weight;**
 - **chromatic aberration cannot be eliminated**
 - **light absorbed by lens**
 - **to achieve large $f/$ numbers, telescope is long and so requires massive supports and large domes**

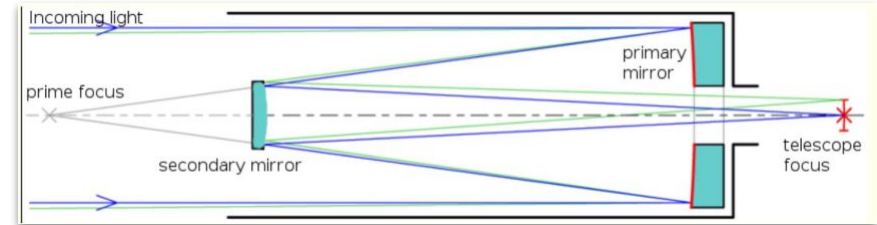


TELESCOPE CONFIGURATION

Reflectors Telescopes (mirrors):

- **Pro:**

- mirror can be supported from the back and gravitational deformations corrected using active optics
- no chromatic aberration
- mirrors can have higher reflectivity than lenses have transparency
- by having multiple reflections inside telescope tube, telescope can be shorter to achieve same $f/$ number and so requires less massive supports and domes

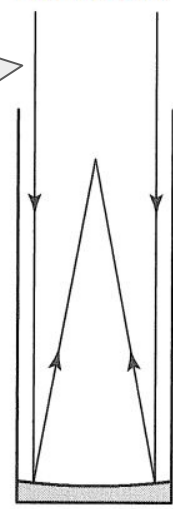


TELESCOPE CONFIGURATION

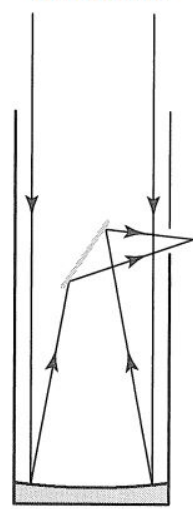
Different focal configurations for a reflecting telescope:

Wide-field camera are deployed at the prime focus as to have the shortest focal length

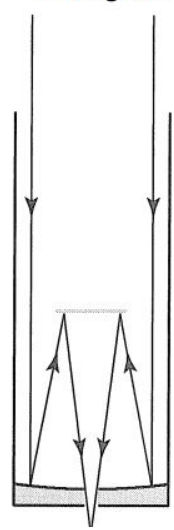
Prime Focus



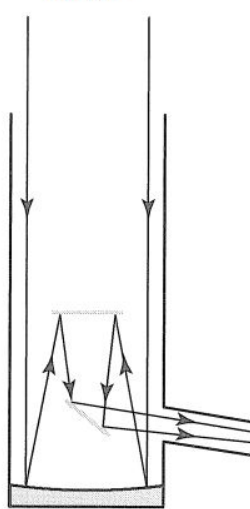
Newtonian



Cassegrain



Coudé



Coudé (or Nasmyth) focus has a very long focal length and uses an additional mirror to transport the focus to a nearby instrument, typically a very stable spectrograph in a temperature controlled room

If the secondary mirror is curved rather than flat, the focal length of the telescope can be changed

NORTHERN TELESCOPES

Table 5.1 Large ground-based optical telescopes in the northern hemisphere

Latitude	Altitude [m]	Site	Country	Diameter [m]	Remarks	Date
47°N	2 070	Zelenchuskaya (Caucasus)	Russia	6	Altazimuth mount	1972
42°N	2 500	Xing Long	China	4	LAMOST siderostat	2007
37°N	2 160	Calar Alto (Spain)	Germany and Spain	3.5		1981
34°N	1 706	Palomar (California)	USA	5	First VLT	1948
32°N	2 130	Kitt Peak, Arizona	USA	3.8	Mayall	1974
	3 266	Mt. Graham, Arizona	USA, Italy, Germany	2 × 8.2	LBT	2007
30°N	2 076	Mt. Locke (Texas)	USA	9.2	Hobby–Eberly fixed elevation	1997
28°N	2 370	La Palma (Canaries)	UK	4.2	WHT (Herschel)	1984
			Spain	10.4	GranTeCan	2008
19°N	4 200	Mauna Kea (Hawaii)	UK	3.8	Infrared UKIRT	1979
			Canada, France, Hawaii	3.6	CFHT	1974
			USA (CalTech)	2 × 10	Keck I and II	1994
			Japan	8.4	Subaru	1999
			USA (NSF)	8.0	Gemini N	1999

SOUTHERN TELESCOPES

Table 5.2 Large ground-based optical telescopes in the southern hemisphere

Latitude	Altitude [m]	Site	Country	Diameter [m]	Remarks	Date
23°S	2 650	C. Paranal (Chile)	Europe	4 × 8.2	VLT	1998
				4	VISTA	2008
29°S	2 280	Las Campanas (Chile)	USA	2 × 6	Magellan	2002
29°S	2 430	La Silla (Chile)	Europe (ESO)	3.6		1977
				3.5	NTT	1989
30°S	2 700	C. Tololo (Chile)	USA	4	Blanco	1974
	2 738	C. Pachon (Chile)	USA	8.1	Gemini S	2001
32°S	1 500	Sutherland (South Africa)	Brazil and USA	4.1	SOAR	2005
			South Africa and others	11	SALT	2005
34°S	1 165	Siding Springs (Australia)	Australia and UK	3.9	AAT	1974

OPTICAL / NIR DETECTORS: PHOTOGRAPHIC PLATES

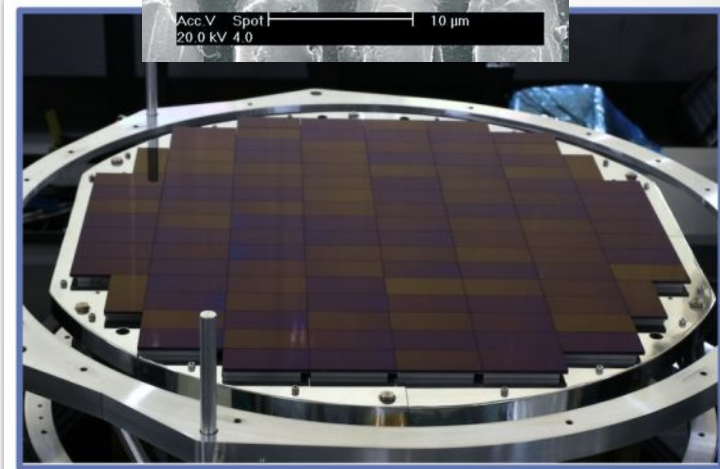
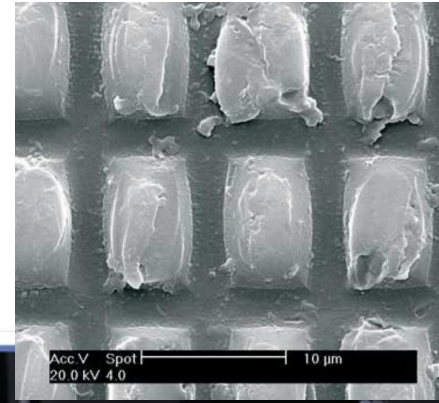
- **Photographic plates have been used to image the sky and obtain spectra of astrophysical sources over the past century**
 - **A light sensitive emulsion is applied to glass plates**
 - **Plates are exposed and each absorbed photon results in a chemical change in a molecule of this emulsion**
 - **plates are then developed in a chemical process**
- **Plates have a non-linear response, because the probability of detecting an incoming photon depends on the density of light-sensitive chemicals in plate. As light is absorbed this density falls and the plate becomes less sensitive**

Coma Cluster in POSS2 Red



OPTICAL / NIR DETECTORS: CCD

- A Charge Coupled Device is a 2D array of silicon pixels that converts incoming photons into stored electric charge. Each pixel acts as a potential well for photo-electrons.
- CCD surface is divided into rows and columns of pixels with characteristic size $\sim 10 \mu\text{m}$; typical sizes are 2048 to 4096 on a side, corresponding to $\sim 2.5 \text{ cm}$
- High linearity and broad wavelength sensitivity have made CCDs the detector of choice on optical astronomy.
- Nowadays large sky cameras are built from large arrays of CCDs, enabling efficient mapping of large portions of the sky

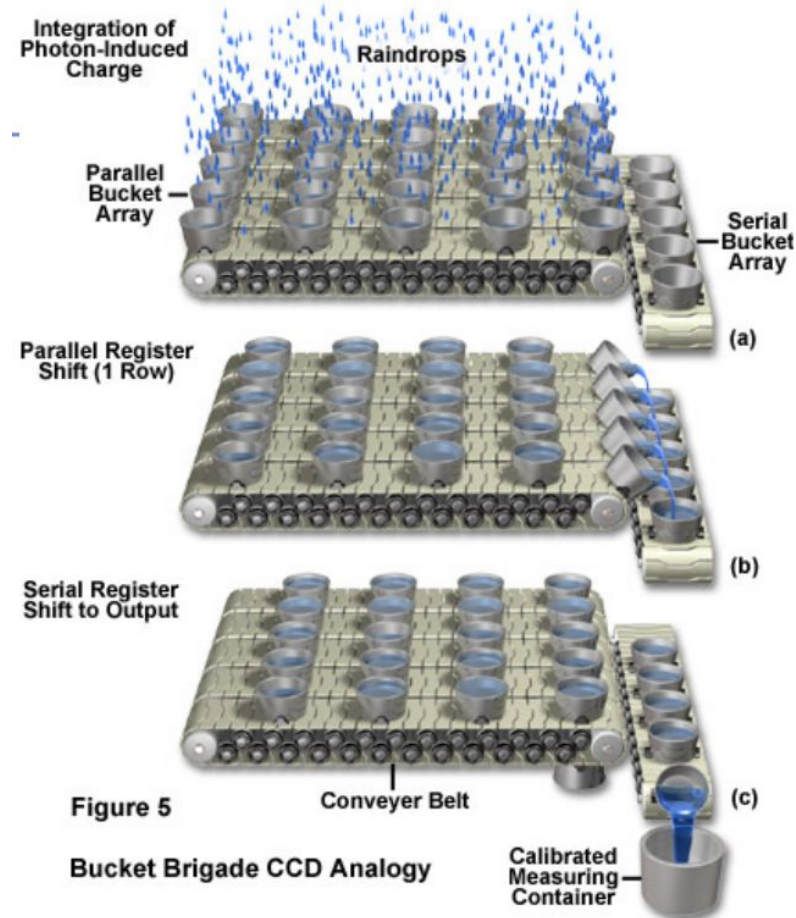
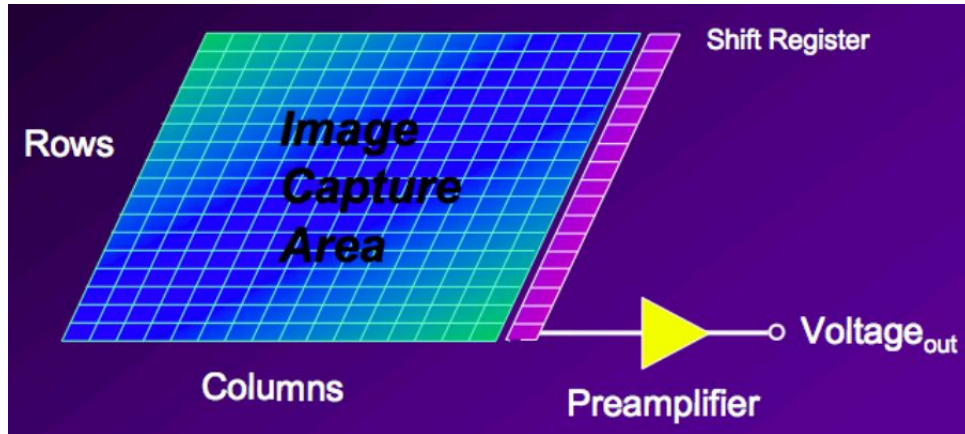


Hyper-Suprime-Cam built
for the Subaru Telescope

OPTICAL / NIR DETECTORS: CCD

Exposure and Readout:

- Incoming photon with $h\nu > E_g = 1.11\text{eV}$ creates an electron-hole pair in silicon
- Electrons are trapped in pixel wells during the exposure time \rightarrow Total charge \propto incident flux \times exposure time
- After exposure, charges are shifted pixel-to-pixel along columns in serial read-out register
- The output current is amplified and measured
- Digitize output voltage (typically 16-bit ADC)
- Store data (1 detector pixel \rightarrow 1 image pixel)



OPTICAL / NIR DETECTORS: CCD

CCDs are:

- extremely sensitive with quantum efficiencies = $(\# e^- \text{ collected})/(\# \text{ incoming } \gamma)$ reaching 80% or higher
 - For comparison photographic plates or eye have QE $\sim 1\%$
- Sensitive to photons over a broad range of energies ($>1.11\text{eV}$ or $<1.1 \mu\text{m}$, the silicon band gap)
- have a linear response over dynamic range of 10^5 (read noise floor of $1\text{-}2 e^-$ and full well capacity of $\sim 10^5 e^-$)
 - Compare to photographic plates that are linear over dynamic range of 10^2

These properties allow:

- Quantitative astrometric measurements of extended sources
- Time-domain astronomy
- Wide-field surveys
 - E.g. Sloan Digital Sky Survey, Pan-STARRs1, Dark Energy Survey, Euclid, LSST

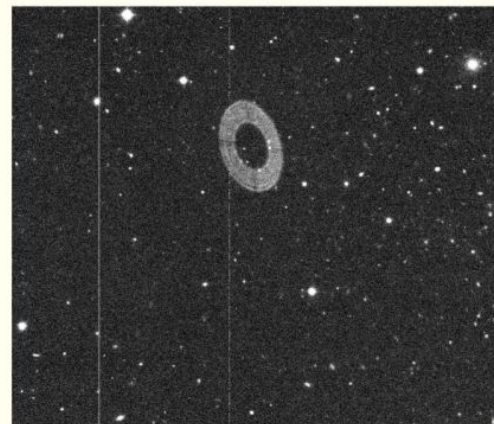
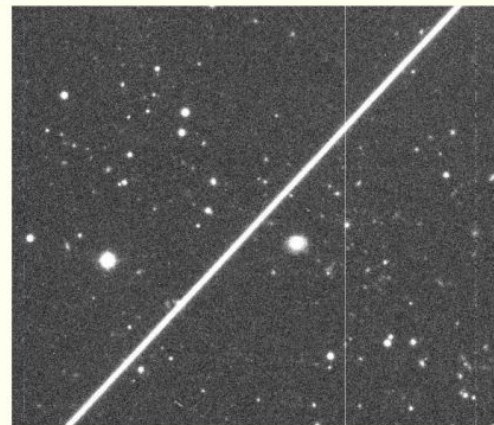
OPTICAL / NIR DETECTORS: CCD

Raw images from a given CCD typically have unwanted structures:

- Read-outs might have different bias level
- Saturation or spikes around bright sources
- Electronic artifacts, e.g. dead or bright columns
- In addition to cosmic rays, scattered light, satellite trails, etc etc

Single epoch (exposure) images need to be calibrated to remove all these effects

Coadded images are science ready data which combine calibrated single epoch images to create high quality images.



OPTICAL / NIR DETECTORS: CMOS

What about IR?

- The silicon band gap makes it impossible to use standard silicon-based CCD at wavelengths beyond $\sim 1 \mu\text{m}$

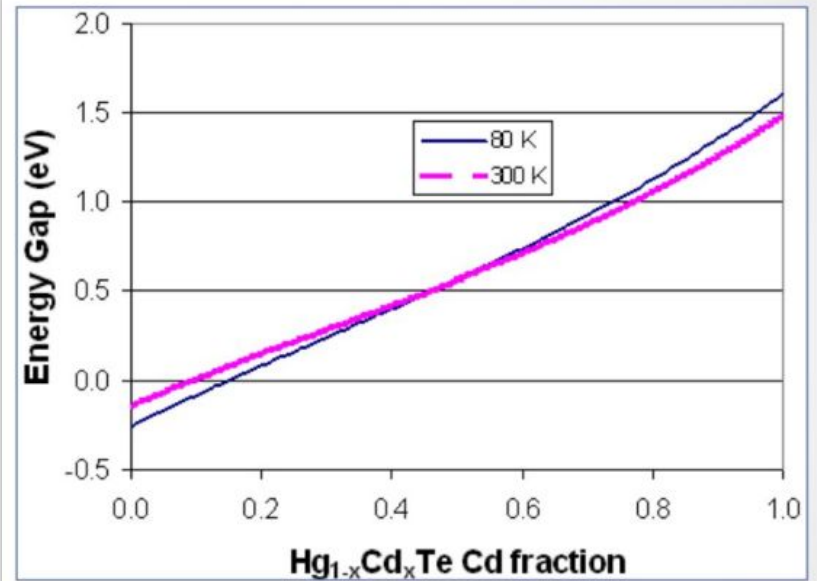
Hybrid Complementary Metal Oxide Semiconductor (CMOS) devices are well suited for infrared photon detection



Hubble IR Image of Tarantula Nebula
IJH bands Wide Field Camera 3 and
Advanced Camera for Surveys

OPTICAL / NIR DETECTORS: CMOS

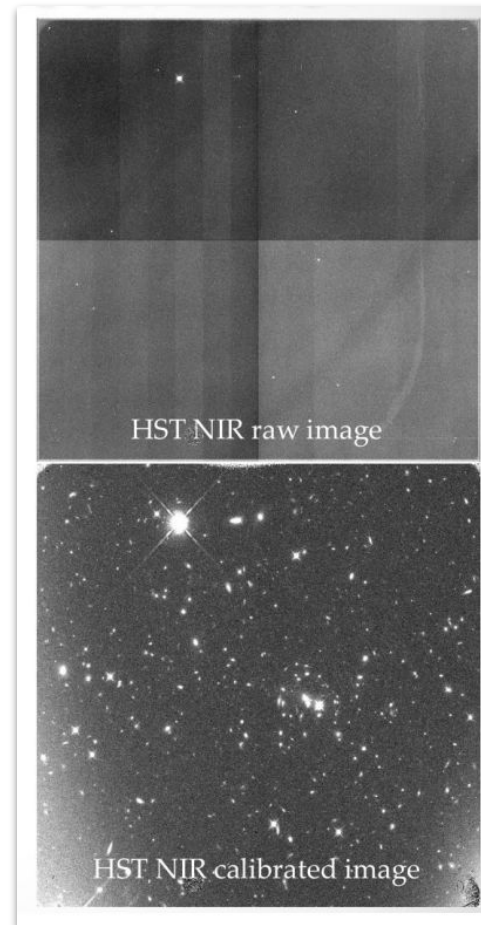
- CMOS detectors are solid-state imaging arrays where each pixel contains its own readout electronics, i.e. charge is converted to voltage locally, not shifted across the array
 - Each pixel includes:
 - Charge-to-voltage converter
 - Amplifier
 - No charge transfer across the detector
 - High readout speed
- CMOS couple photodiode made from material that is photosensitive at the desired wavelength (HgCdTe) to a silicon readout circuit (Hybrid devices)
- Sensitivity to low energy photons then requires low operating temperatures (<100 K) to suppress thermal noise (or dark current)



HgTe is semimetal and CdTe is semiconductor. By adjusting Cd fraction one can tune the wavelength sensitivity of the HgCdTe arrays

OPTICAL / NIR DETECTORS: CMOS

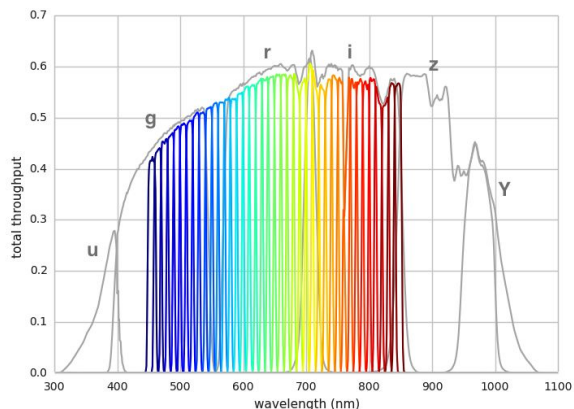
- **Ground based IR images look like noise:**
 - **Observations are usually background limited: the sky is so bright in the IR band that the exposures must be very short (~10s)**
 - **Narrow atmospheric windows (J, H, K bands) due strong molecular absorption (H_2O , CO_2 , CH_4)**
 - **Large series of images are taken with small dithers**
 - **Sky is subtracted and images coadded as with CCD images**
- **From space the background is much lower (dominated by zodiac light), but there is a higher particle background (cosmic rays)**



OPTICAL / NIR

Photometric Passbands:

- In optical and NIR photometry one often encounters measurements in particular passbands. The table on the right is a list of the standard broadband filters
- Narrow band filters are often used to seek particular spectral lines or features and/or improve constraints on the spectral energy distribution of the source

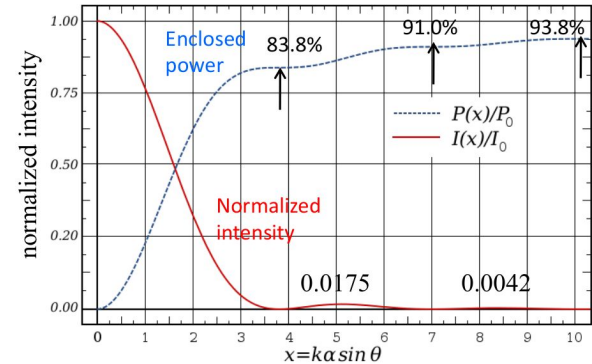
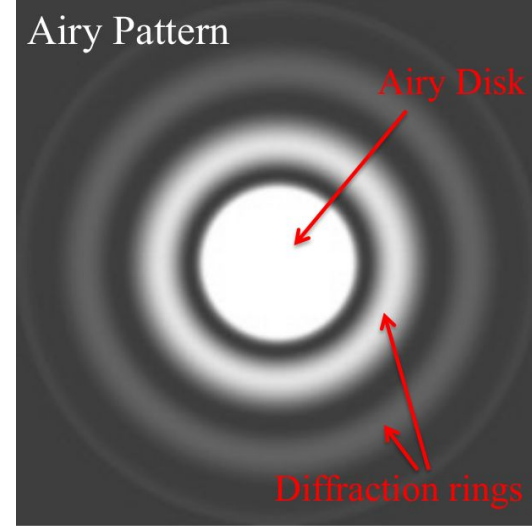
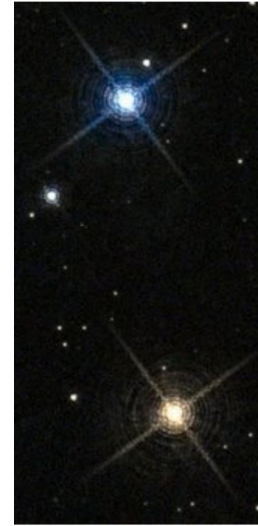


40 narrow bands of the PAU camera

Band	λ_{mid}	$\Delta\lambda$
U	365	66
B	445	94
V	551	88
R	658	138
I	806	149
Z	900	
Y	1020	120
J	1220	213
H	1630	307
K	2190	390
L	3450	472
M	4750	460

OPTICAL / NIR: GROUND VS SPACE

- For space-based (or small ground-based) telescopes the angular resolution is limited by the diffraction of the telescope aperture
- The diffraction pattern produced by a circular aperture is known as the Airy pattern, which comprises a bright central disk (83.3% of the energy) surrounded by much dimmer diffraction rings.
- The first minima, which define the Airy disk, occurs at: $\theta = 1.22 \lambda / D$



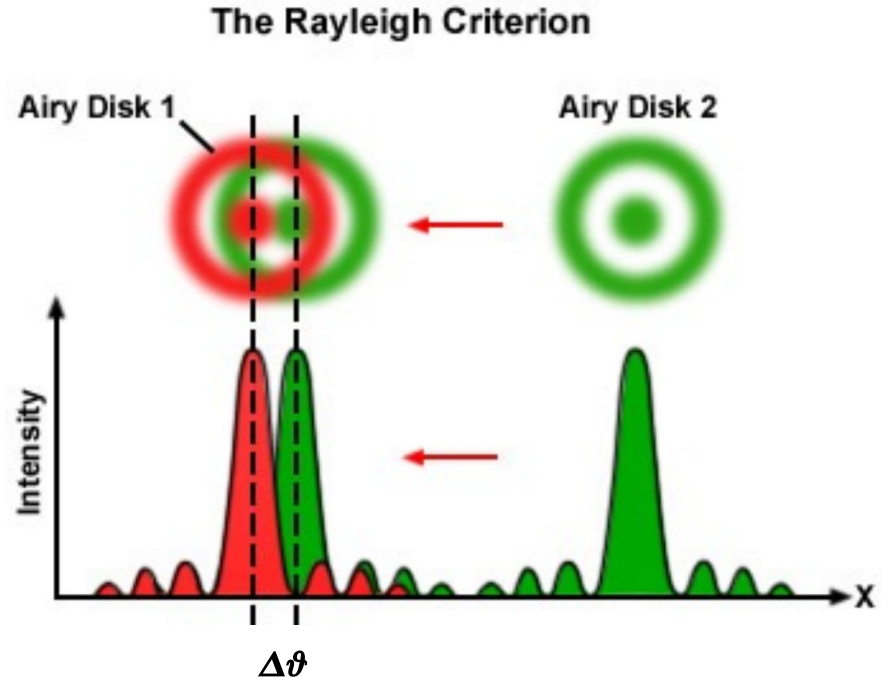
OPTICAL / NIR: GROUND VS SPACE

- The Rayleigh criterion for resolving two point sources requires:

$$\Delta\theta > 1.22 \lambda / D$$

- Rayleigh criterion corresponds closely to the diameter of the Airy disk as measured at full-width half-maximum (FWHM), which provides a more convenient measure of the angular resolution
- Angular resolution at optical wavelengths ($0.5 \mu\text{m}$) of human eye at night is about $20''$.

- 2.4 m, $\theta_{\text{min}} = 0.05''$ (Hubble Space Telescope)
- 4 m, $\theta_{\text{min}} = 0.03''$ (Canadian-France-Hawaii Telescope)
- 8.2 m, $\theta_{\text{min}} = 0.015''$ (Subaru Telescope)

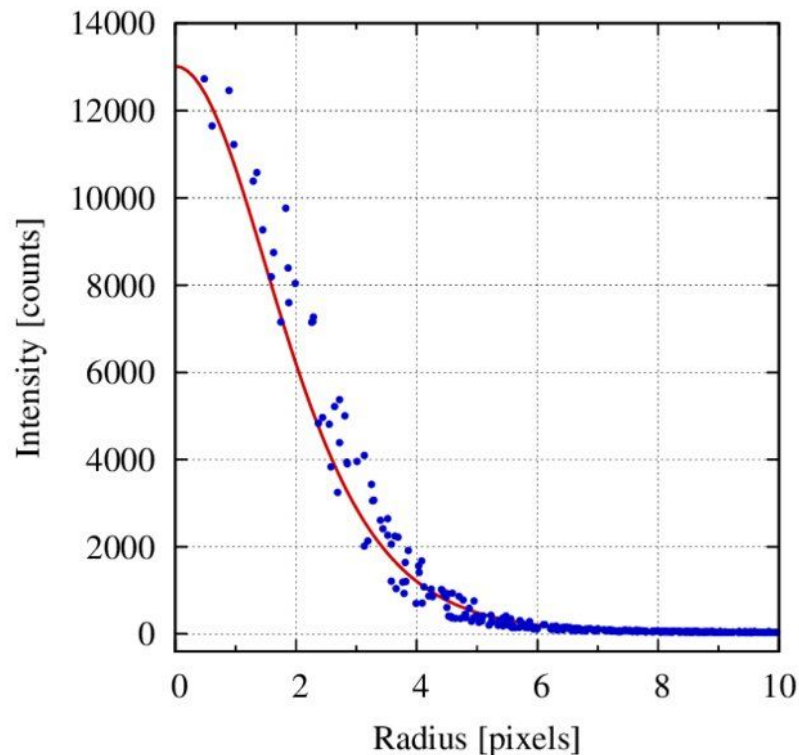


OPTICAL / NIR: GROUND VS SPACE

- For large ground-based telescopes the Point-Spread Function (PSF) is a function of atmosphere, rather than telescope optics.
- The PSF is well described by a Moffat profile with free parameters R (width) a β (shape)

$$I(r) = \frac{I_0}{(1 + r^2/R^2)^\beta} + B$$

- The “seeing” disk, which define the resolution of ground-based telescope, corresponds to the FWHM of the PSF. A seeing of 0.5” is very good, 2” is bad (e.g. weak lensing measurements requires < 1 ”). Without corrections all telescopes with $D > 25\text{cm}$ are limited by atmospheric seeing \rightarrow adaptive optics

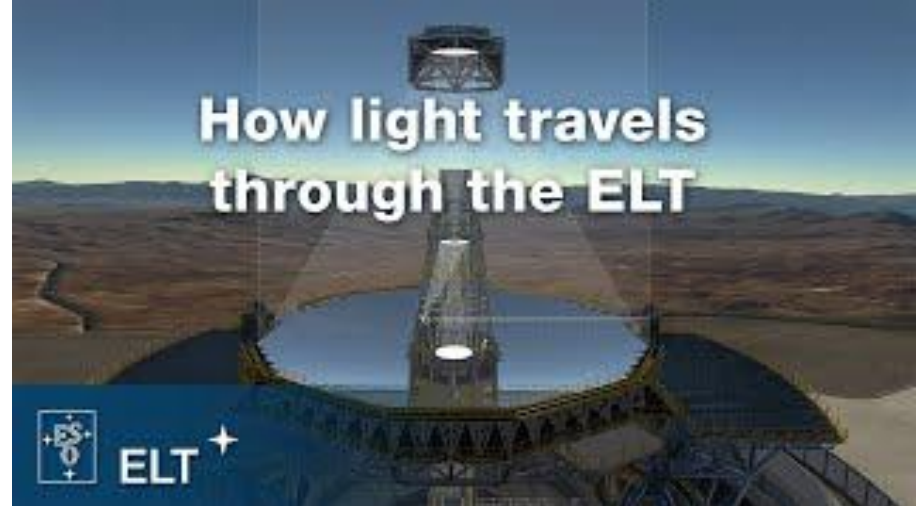
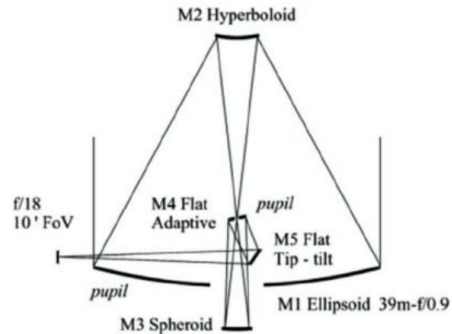
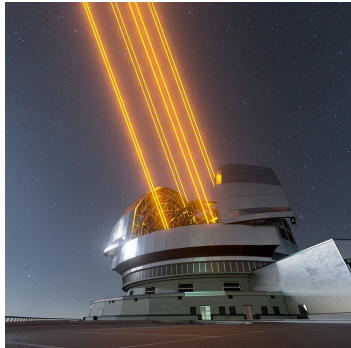


OPTICAL / NIR TELESCOPES: ELT



Extremely Large Telescope:

- Primary 39m
- FoV 10 arcmin
- Adaptive optics
- 6 laser guide stars
- 2 Nasmyth platforms for instrumentation
- First light 2029

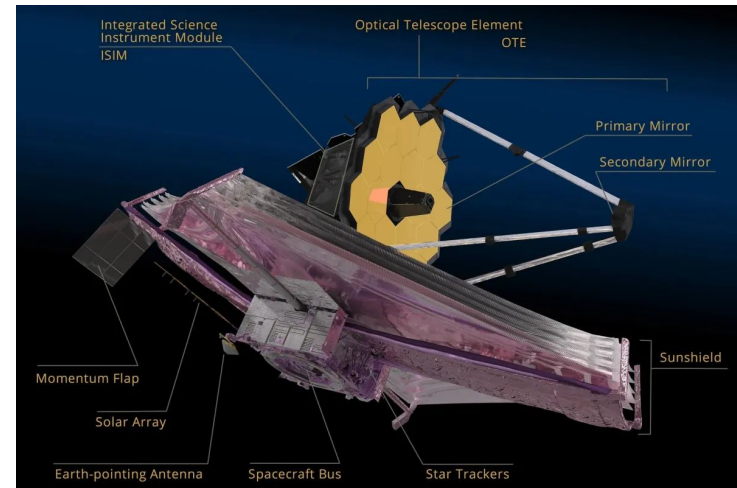


OPTICAL / NIR TELESCOPES: JWST

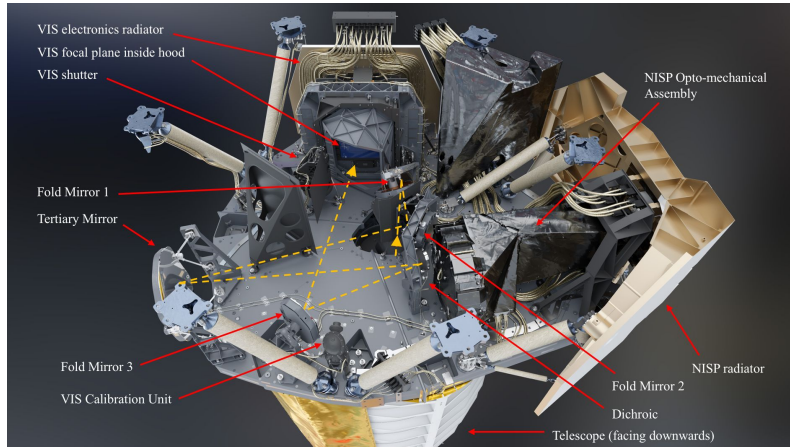


James Webb Space Telescope:

- Primary 6.5m
- FoV ~4 arcmin
- NIR/MIR camera + NIR spectrograph
- Launched 2021

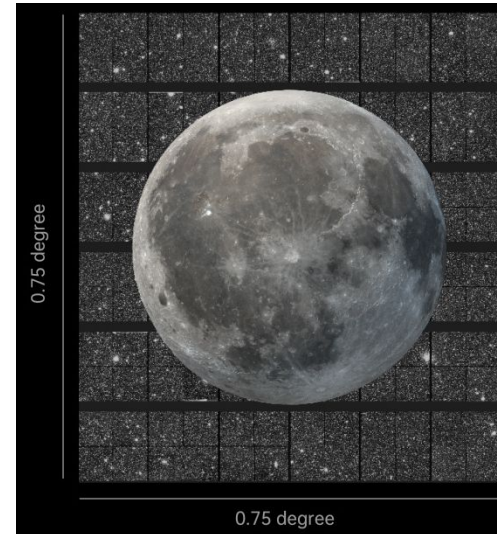
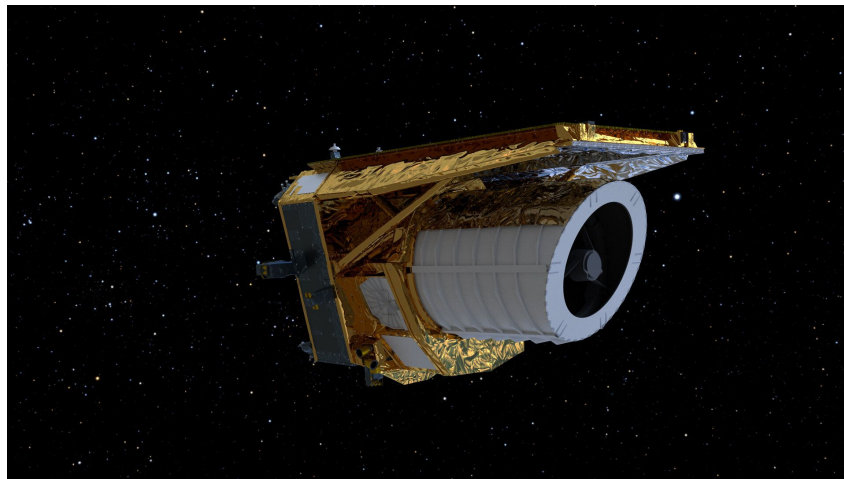


OPTICAL / NIR TELESCOPES: Euclid



Euclid:

- Primary 1.2m
- FoV $\sim 0.5 \text{ deg}^2$
- Optical/NIR
- Imaging and spectroscopy
- Launched 2023

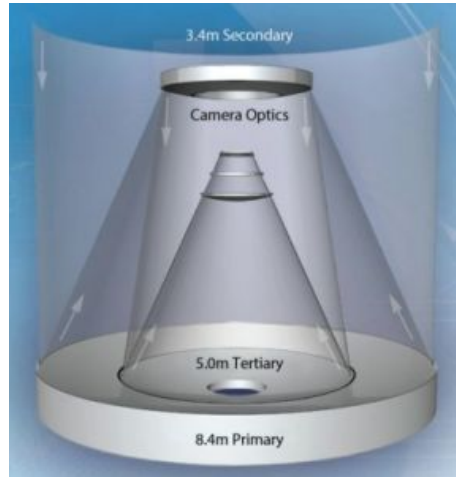


OPTICAL / NIR TELESCOPES: LSST Rubin

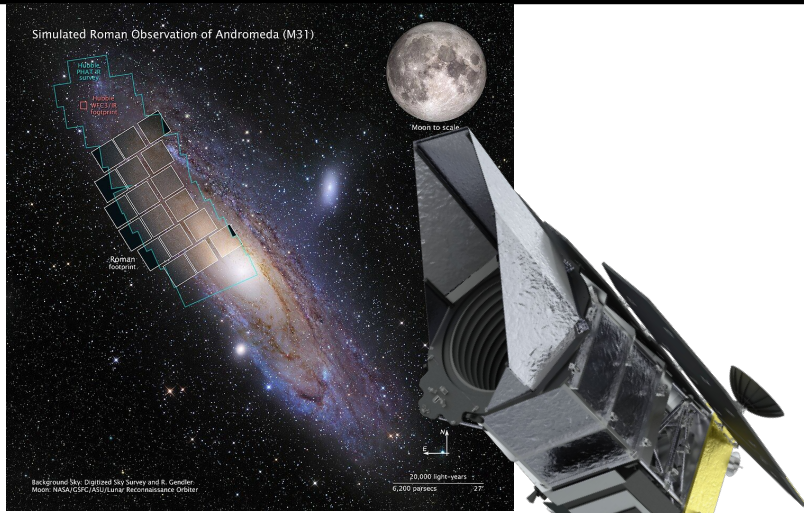


LSST - Vera Rubin Observatory:

- Primary 8.4m
- FoV $\sim 10 \text{ deg}^2$ ($\sim 40 \times$ full moon)
- Optical/NIR and time domain
- First light 2025



OPTICAL / NIR TELESCOPES: ROMAN & CSST



Roman Space Telescope (NASA):

- Launch: late 2020s
- Primary mirror: 2.4m
- FoV $\sim 0.28 \text{ deg}^2$ ($\sim 100 \times$ HST)
- NIR: $0.5\text{-}2.3 \mu\text{m}$
- Coronagraph Instrument

Cosmology and exoplanet science



China Space Station Telescope (CNSA):

- Launch: late 2020s
- Primary mirror: 2.0m
- FoV $\sim 1.1 \text{ deg}^2$ ($\sim 300 \times$ HST)
- Resolution: $\sim 0.15''$
- Optical/NIR: $255 \text{ nm} - 1 \mu\text{m}$
- Multiband imaging (7 bands)
- Slitless spectroscopy

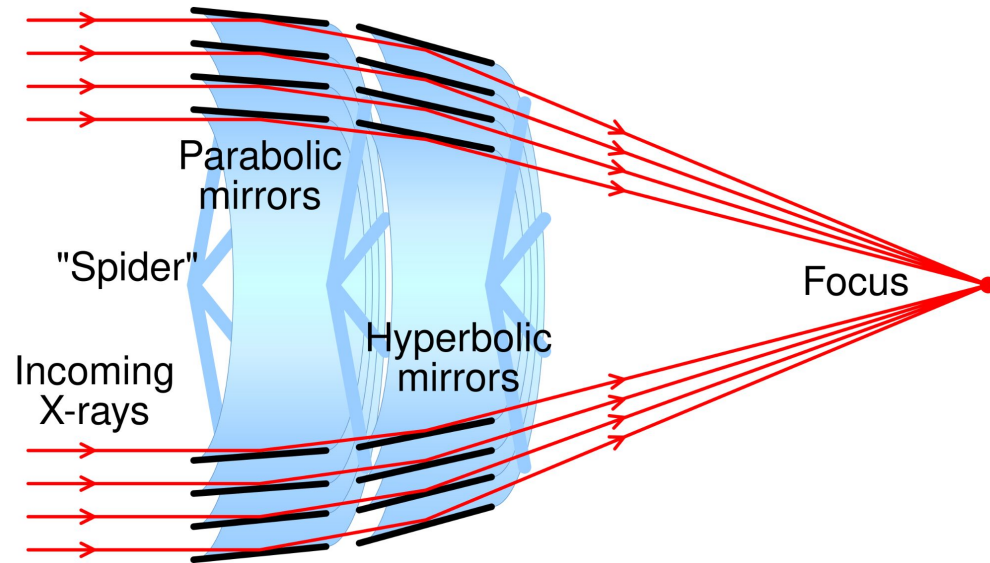
X-RAY AND γ TELESCOPES

X-RAY REFLECTIVE OPTICS

X-ray tend to penetrate and eventually get absorbed in most materials without significant change of direction. X-ray optics thus require grazing incidence angles ($\sim 89^\circ$ from the normal) and multilayer coating.

Wolter X-ray telescope:

- parabolic mirror followed by a reflection off a hyperbolic mirror
- design offers the possibility of nesting several telescopes inside one another, thereby increasing the useful reflecting area.
- X-ray mirror quite massive, focal lengths are long, FoV small
- Off-axis aberrations controllable, but problematic



X-RAY IMAGE QUALITY

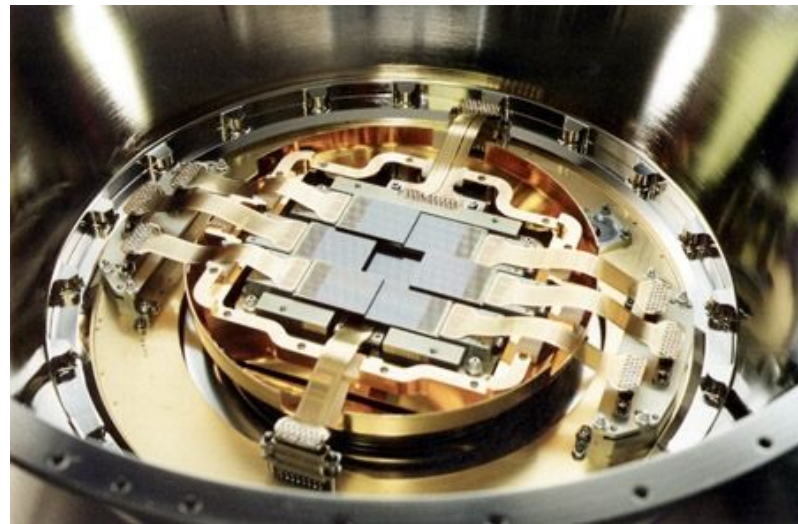
- Efficiency of scattering depends on photon energy: there is an inverse relation between critical angle for total reflection and radiation energy → Higher energy photons scatter only at the highest incidence angles → This effect also limit the effective energy range of X-ray telescope to 0.1-15 keV (soft X-ray)
- Image quality:
 - Not related to diffraction limit (given the small wavelength it would be incredibly small)
 - Defects in crystalline structure of metallic mirror surfaces and alignment on the concentric telescopes are key to the delivered resolution

Angular resolution (PSF width) of X-ray observatories as a function of off-axis angle

Observatory	Energy [keV]	0'	5'	10'	20'
ROSAT	1	3''	3''	7''	26''
XMM	<2.5	20''	-	-	-
Chandra	-	<1''	2''	5''	20''

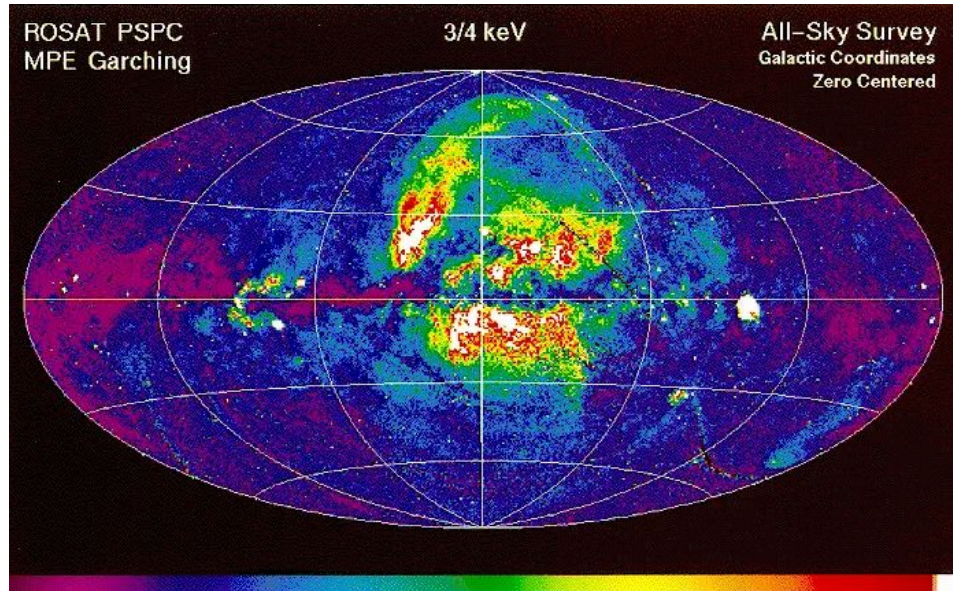
X-RAY DETECTORS

- Most existing X-ray telescopes – e.g. XMM and Chandra – use CCD detectors, similar to those in visible-light cameras. Each X-ray photon produces enough charge on the CCD that it can be used as photon-counting spectrometers, and X-rays have their energies measured on read-out.
- Specifically:
 - Each incoming photon produces many electrons rather than a single e^-
 - Event is typically spread over multiple neighboring pixels
 - Mean position of charge distribution gives the incoming position of the X-ray photon
 - The sum of the charge gives the energy of the X-ray photon
 - Detectors must be read quickly; two events overlapping in pixel space (pile-up) cannot be disentangled

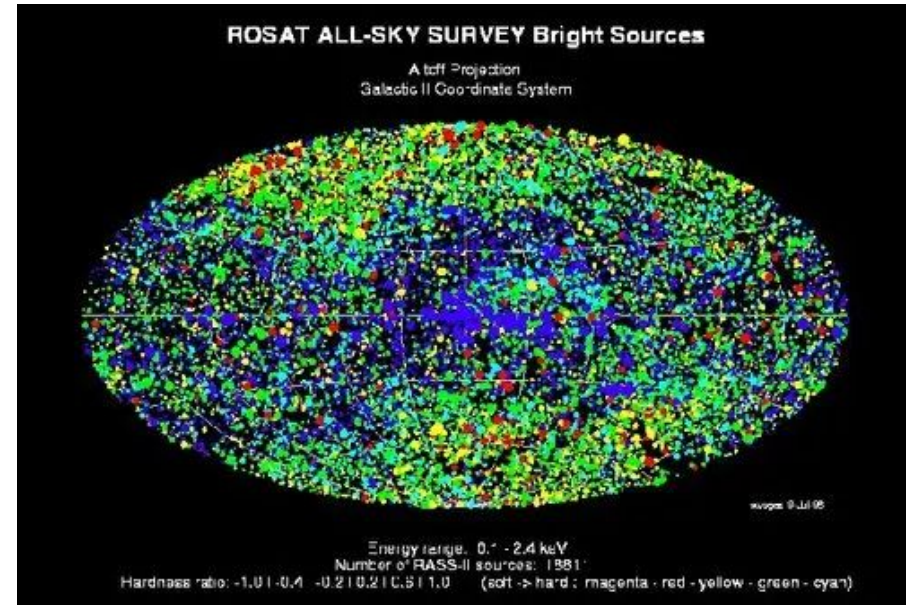


The CCDs of one of the MOS cameras of XMM-Newton.

X-RAY ROSAT SKY



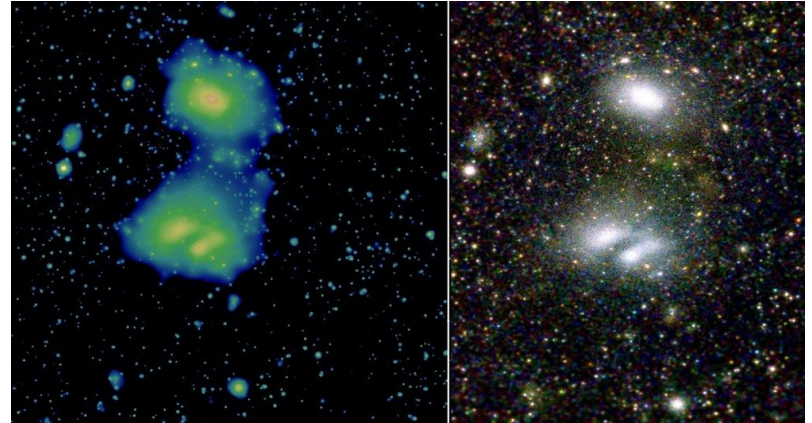
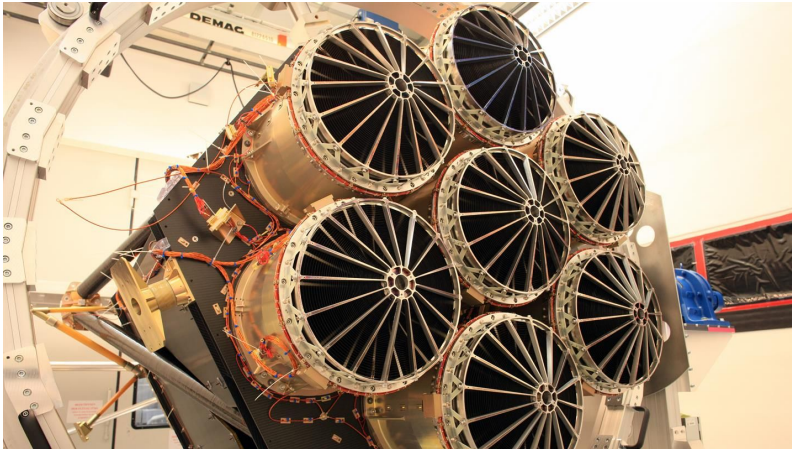
ROSAT sky map for the energy range 0.5-0.9 keV (3/4 keV band) The X-rays are emitted mainly by some million-degree gases such as stellar coronae, supernova remnants, superbubbles, and the hot plasma of the galactic nucleus. Aside from this, one can recognize a weak isotropic extragalactic radiation from the superposition of unresolved active galaxies and clusters of galaxies.



The 18,811 sources in this map are catalogued, with a limiting ROSAT PSPC count rate of 0.05 cts/s in the 0.1-2.4 keV energy band.

eROSITA SURVEY MISSION

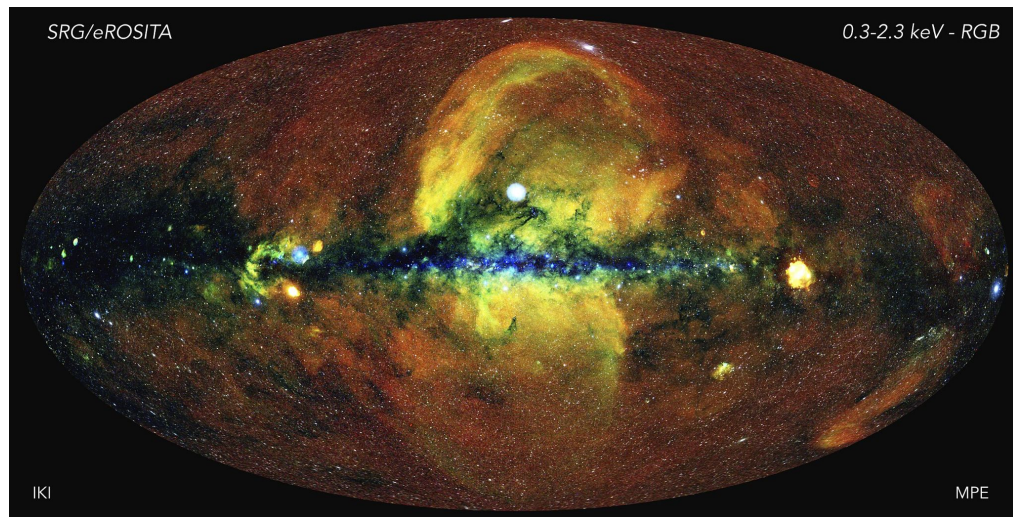
- 7 independent telescopes:
 - Each with ~30 concentric, nested Wolter grazing incidence mirrors
 - Each has 1 deg diameter of FoV
 - Each has collecting area of ROSAT
 - Each delivers ~30" angular resolution
 - Each is coupled to a position and energy sensitive detector



These eROSITA images show the two interacting galaxy clusters A3391, towards the top of the images, and the bimodal cluster A3395, towards the bottom, highlighting eROSITA's excellent view of the distant Universe. In the left-hand image, the red, green and blue colours show the three different energy bands observed by eROSITA.. The eROSITA observations also show hundreds of point-like sources, revealing either distant supermassive black holes or hot stars in the Milky Way.

eROSITA SURVEY MISSION

- All Sky Survey
 - eROSITA operate at L2
 - Satellite rotates around axis defined by it and the Sun, scanning the sky that is $\sim 90^\circ$ from the Sun
 - Complete sky survey each 6 months due to Earth's orbit
- Launched by Roscosmos on 13 July 2019
- It began collecting data in October 2019. Due to the breakdown of institutional cooperation between Germany and Russia after the invasion of Ukraine, the instrument stopped collecting data on February 26, 2022.



The first all-sky survey was completed on June 11, 2020, cataloging 1.1 million sources, including mostly Active Galactic Nuclei (77%), stars with strong, magnetically active hot coronae (20%) and clusters of galaxies (2%), but also bright X-ray binaries, supernova remnants, extended star-forming regions as well as transients such as Gamma-Ray Bursts. The map includes extended features of the Milky Way, including mushroom-like bubbles and absorbing galactic gas in the disk (blue). (Credit wikipedia)

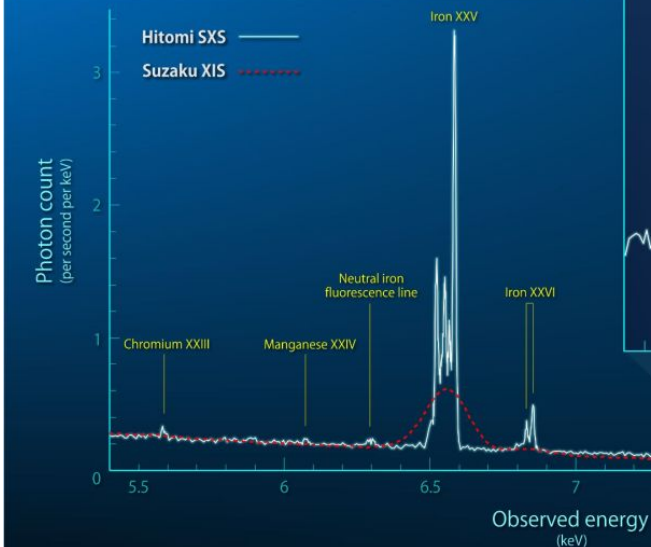
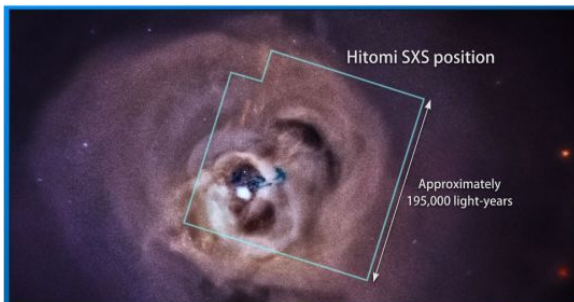
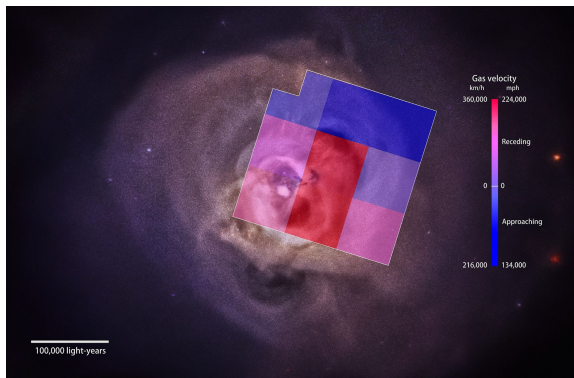
Astro-H (HITOMI): 5 eV vs 100/150 eV

- Instruments:

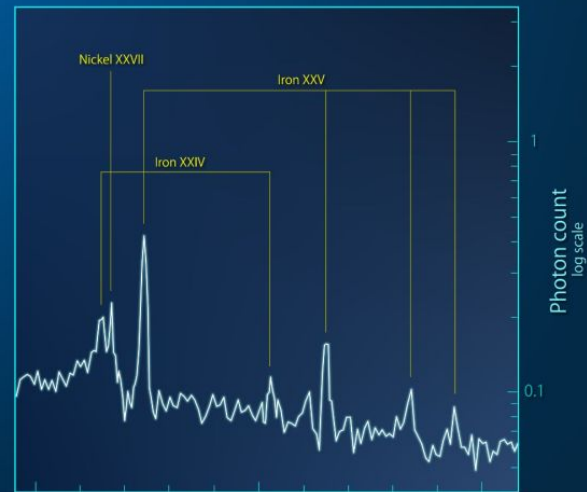
- 2 soft X-ray telescopes (0.4-12 keV) for high resolution spectroscopy (5 eV!)
- 2 hard X-ray telescopes (5-80 keV)
- 2 soft γ ray detectors (60-600 keV)

- Mission duration:

- 3 years (planned)
- ~37.5 days (achieved)



Perseus Galaxy Cluster X-ray Spectra



Launch on Sept 2023



Key questions



How did clusters of galaxies form and evolve?



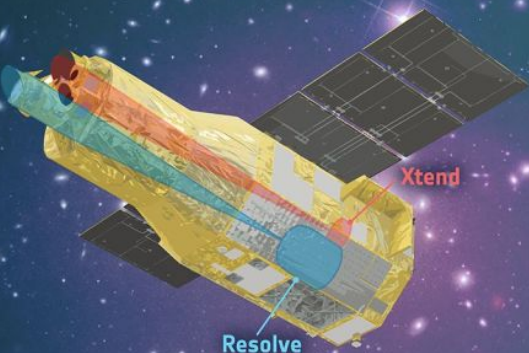
How did the Universe produce and distribute chemical elements?



What does the structure of spacetime look like under intense gravity?



How do massive black holes affect star formation in their host galaxies?



Resolve

Xtend

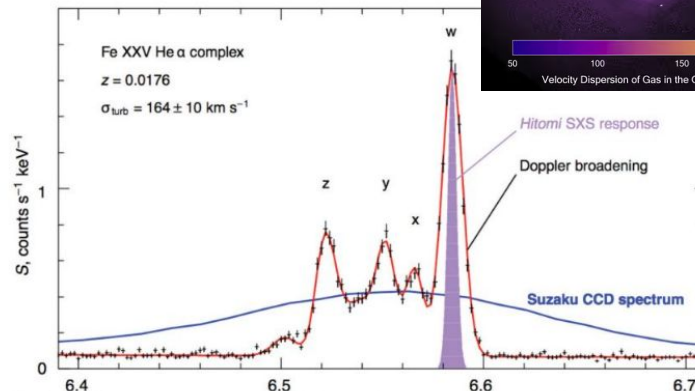
Two science instruments



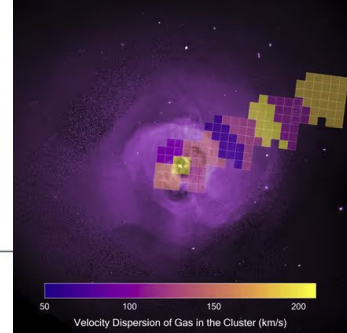
Resolve: measuring the temperature and dynamics of X-ray emitting objects



Xtend: imaging extended X-ray emitting celestial sources and their surroundings



The Hitomi spectrum of the Perseus Cluster, showing the power of microcalorimeter X-ray spectroscopy. The previous best X-ray spectrum of this object is the Suzaku spectrum, shown in blue.



Parameter	Requirement	Goal
Energy Resolution	7 eV (FWHM)	5.0 eV
Energy Scale Accuracy	± 2 eV	± 0.5 eV
Residual Background	2×10^{-3} counts/s/keV	$< 1 \times 10^{-3}$ counts/s/keV
Field of View	2.9×2.9 arcmin	same, by design
Angular Resolution	1.7 arcmin (HPD)	1.2 arcmin
Effective Area (1 keV)	> 160 cm ²	250 cm ²
Effective Area (6 keV)	> 210 cm ²	312 cm ²
Cryogen-mode Lifetime	3 years	4+ years
Operational Efficiency	$> 90\%$	$> 98\%$

Fermi GAMMA-RAY TELESCOPE

- **Instruments:**

- LAT: imaging gamma-ray detector (20 MeV to 300 GeV) with a field of view of about 20% of the sky
- GBM: 14 scintillation detectors (8 keV - 30 MeV) can detect gamma-ray bursts in that energy range across the whole of the sky not occluded by the Earth.

- **Key scientific objectives:**

- Understand the mechanisms of particle acceleration in AGN, pulsars, and supernova remnants.
- Resolve the gamma-ray sky: unidentified sources and diffuse emission.
- Determine the high-energy behavior of gamma-ray bursts and transients.
- Probe dark matter (e.g. by looking for an excess of gamma rays from the center of the Milky Way) and early Universe.

Fermi LAT

Public Data Release:

All γ -ray data made public within 24 hours (usually less)

Fermi LAT Collaboration:

~400 Scientific Members,
NASA / DOE & International Contributions



Si-Strip Tracker:

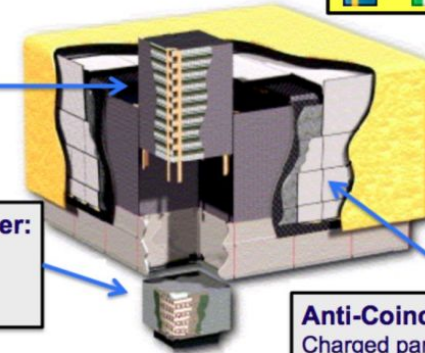
convert $\gamma \rightarrow e^+e^-$
reconstruct γ direction
EM v. hadron separation

Hodoscopic CsI Calorimeter:

measure γ energy
image EM shower
EM v. hadron separation

Sky Survey:

With 2.5 sr Field-of-view LAT
sees whole sky every 3 hours



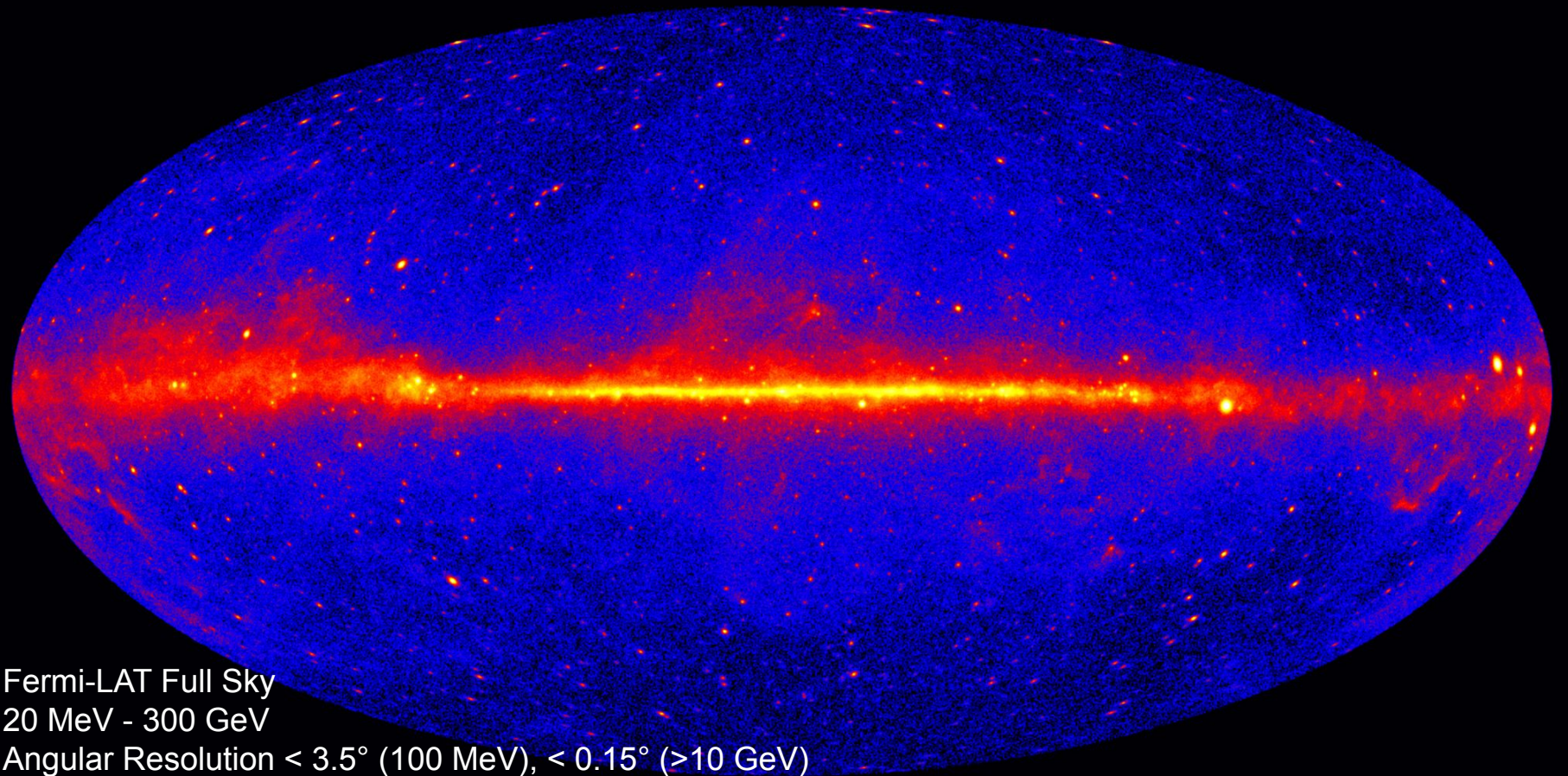
Anti-Coincidence Detector:

Charged particle separation

Trigger and Filter:

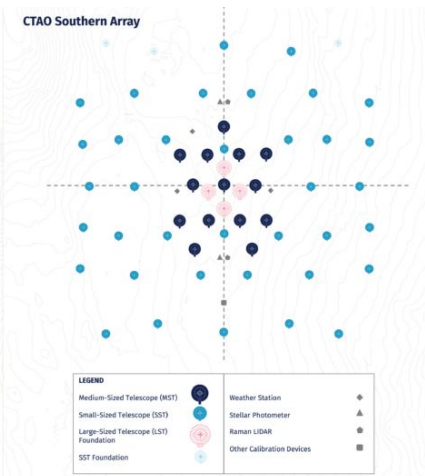
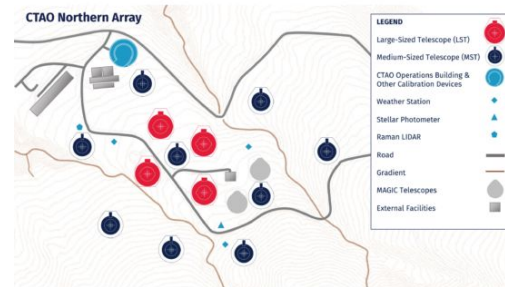
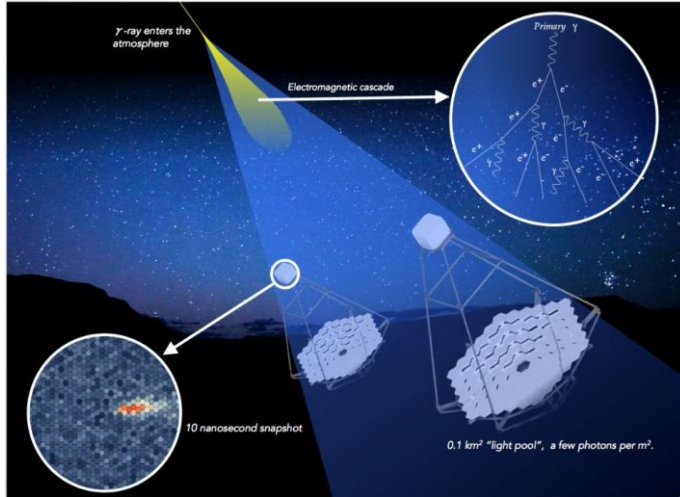
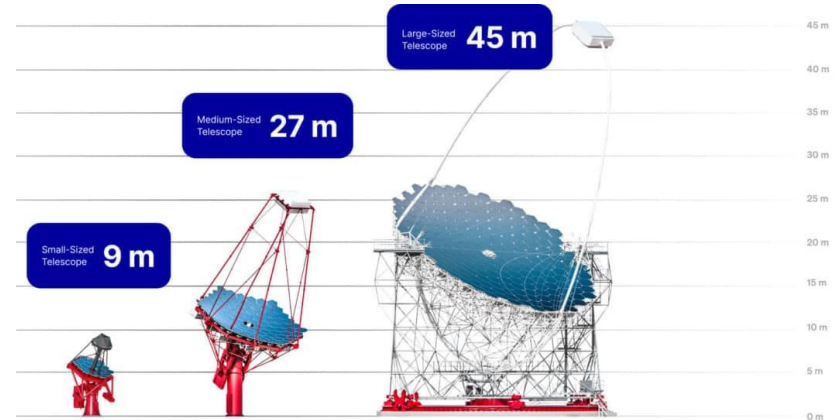
Reduce data rate from ~10kHz
to 300-500 HZ

Fermi GAMMA-RAY TELESCOPE



CHERENKOV TELESCOPE ARRAY OBSERVATORY

- **CTAO:** new generation of ground-based gamma-ray instruments in the energy range ~ 10 GeV to about 300 TeV
- Two arrays of imaging atmospheric Cherenkov telescopes:
 - Southern site (Atacama desert): 4 LST + 25 MST + 70 SST (20 GeV - 300 TeV)
 - Northern site (La Palma): 4 LST + 15 MST (20 GeV - 20 TeV)
- Angular resolution: $\leq 0.05^\circ$
- Energy resolution: $\sim 10\%$



CHERENKOV TELESCOPE ARRAY OBSERVATORY

Particle shower:

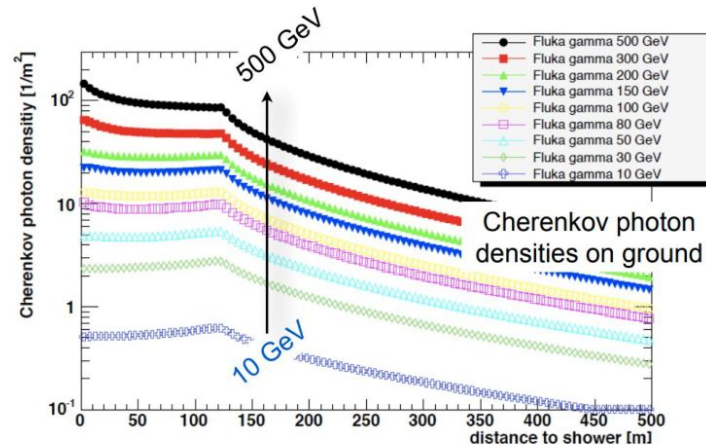
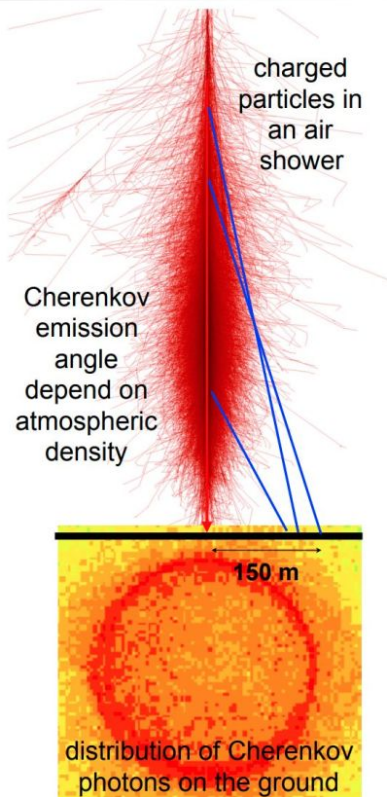
- Primary γ -ray interacts in the upper atmosphere and produces an electromagnetic air shower
- Relativistic charged particles emit Cherenkov light (coherent optical/near-UV emission, $\sim 300\text{--}600\text{ nm}$)

Detection:

- Cherenkov light forms a **nanosecond optical flash**
- Light pool on the ground: **$\sim 120\text{--}250\text{ m}$ diameter**
Telescopes image the shower using **fast photodetectors**

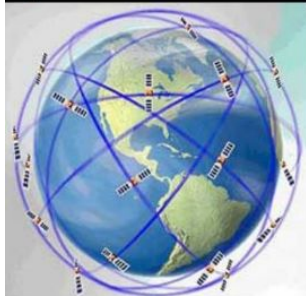
Array:

- Allows to reconstruct shower geometry
- Improve angular resolution
- Suppress hadronic background



Cherenkov light from air showers:
weak ($\sim 10\text{ ph/m}^2$), short ($\sim\text{ns}$),
blue ($300\text{--}550\text{nm}$) flash of light

HERMES MISSION



The HERMES mission

High Energy Rapid Modular Ensemble of Satellites
(a nanosatellite swarm monitor for GRB & High Energy GW counterparts)

GRB statistics

Average GRBs: 300/yr
Bright GRBs: 30/yr
GRB structure: duration $0.2 \div 20$ s, shot noise $\tau = 1$ ms, rate = 100/s

Instrument

N = 50/100 Nano Satellites (Modules) in Low Earth Orbit
Average separation between Modules: 6000 km

Module (weight ≤ 10 kg)

5 Detectors

Field of View of each Detector: 2 steradians
GPS absolute temporal accuracy ≤ 100 nanoseconds
GPS based Module positional accuracy: ≤ 10 m

Detector

Scintillator Crystals: CsI (classic) or LaBr₃ or CeBr₃ (rise – decay: 0.5 – 20 ns)
Photo-detector: Silicon Photo Multiplier (SiPM) or Silicon Drift Detector (SDD)
Effective area: 10×10 cm
Weight: 0.5/1 kg
Energy band: 3 keV – 50 MeV
Energy resolution: 15% at 30 keV
Temporal resolution: ≤ 10 nanoseconds

Mission performance

Accuracy in delays between Average GRB lightcurves of two Modules
(cross correlation techniques): $0.09 \div 8.7 / 0.06 \div 6.1$ μ sec for Average GRBs
Continuous recording of buffered data

Triggered to ground telemetry transmission

IRIDIUM constellation for transmission of TOA of GRB (position after few minutes)

Range of accuracy in positioning of GRB: $0.80 \div 78 / 0.53 \div 54$ arcsec

Modular structure: overall effective area 1 m^2 every 100 modules

